

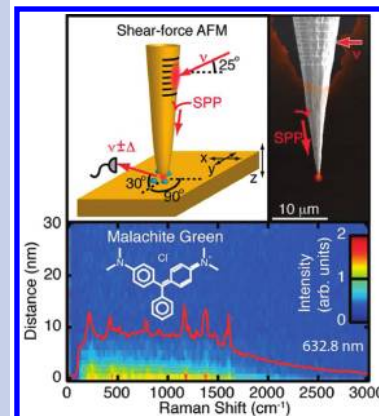
# Adiabatic Tip-Plasmon Focusing for Nano-Raman Spectroscopy

Samuel Berweger,<sup>†,§</sup> Joanna M. Atkin,<sup>†,§</sup> Robert L. Olmon,<sup>†,‡,§</sup> and Markus B. Raschke<sup>\*,†,§</sup>

<sup>†</sup>Departments of Chemistry and Physics and <sup>‡</sup>Department of Electrical Engineering, University of Washington, Seattle, Washington 98195, United States

**ABSTRACT** True nanoscale optical spectroscopy requires the efficient delivery of light for a spatially nanoconfined excitation. We utilize adiabatic plasmon focusing to concentrate an optical field into the apex of a scanning probe tip of  $\sim 10$  nm in radius. The conical tips with the ability for two-stage optical mode matching of the surface plasmon polariton (SPP) grating-coupling and the adiabatic propagating SPP conversion into a localized SPP at the tip apex represent a special optical antenna concept for far-field transduction into nanoscale excitation. The resulting high nanofocusing efficiency and the spatial separation of the plasmonic grating-coupling element on the tip shaft from the near-field apex probe region allows for true background-free nanospectroscopy. As an application, we demonstrate tip-enhanced Raman spectroscopy (TERS) of surface molecules with enhanced contrast and its extension into the near-IR with 800 nm excitation.

**SECTION** Nanoparticles and Nanostructures



Despite ongoing progress in the development of imaging techniques with spatial resolution beyond the diffraction limit, simultaneous spectroscopic implementations delivering chemical specificity and sensitivity on the molecular level have remained challenging. Far-field localization techniques<sup>1,2</sup> can achieve spatial resolution down to 20 nm by point-spread function reconstruction but typically rely on fluorescence from discrete molecular or quantum dot emitters, with limited chemically specific information. Scanning near-field optical microscopy (SNOM)<sup>3,4</sup> provides subdiffraction-limited resolution through the use of tapered fibers or hollow waveguide tips. However, aperture-limited and wavelength-dependent fiber throughput reduces sensitivity, generally making SNOM unsuitable for spectroscopic techniques that have low intrinsic signal levels. In scattering-type SNOM (s-SNOM) (see, e.g., refs 5 and 6 and references therein), external illumination of a sharp (metallic or semiconducting) probe tip can enhance sensitivity, spectral range, and spatial resolution. Chemical specificity can be obtained through the implementation of, for example, IR vibrational s-SNOM,<sup>7,8</sup> tip-enhanced coherent anti-Stokes Raman spectroscopy (CARS),<sup>9</sup> or tip-enhanced Raman scattering (TERS).<sup>10,11</sup> Here the antenna or plasmon resonances of the (noble) metal tips can provide the necessary field enhancement for even single-molecule sensitivity.<sup>12,13</sup> In the standard implementation, however, the direct illumination of the tip apex results in a three-to-four order of magnitude loss in excitation efficiency, related to the *mode mismatch* between the diffraction-limited far-field excitation focus and the desired tens of nanometers near-field localization, as determined by the tip apex radius. The resulting loss in sensitivity, together with a far-field background signal, often limit contrast and may cause

imaging artifacts, presenting challenges for the general implementation of a wider range of spectroscopic techniques in s-SNOM.

A general solution for optical nanoimaging and spectroscopy thus requires a true nanoconfined light source. While this can be achieved through a nanoscopic emitter in the form of a single molecule, quantum dot, or nanostructure<sup>14,15</sup> at the apex of a tip, that approach relies on the quantum efficiency and spectral characteristics of the emitter, and the difficulties of overcoming the intrinsic background and sensitivity limitations with unmatched far-field mode excitation remain. In our implementation, a nanoemitter is generated through *nonlocal* excitation, taking advantage of the effective tip cone radius-dependent index of refraction  $n(r)$  experienced by a surface plasmon polariton (SPP) propagating along the shaft of a noble metal tip.<sup>16,17</sup> The resulting propagation-induced adiabatic SPP focusing into the tip apex region is due to the continuous transformation of the surface mode size. This approach allows for spatially separated SPP coupling and subsequent probe apex excitation with tens of nanometers field confinement over a broad spectral range with high focusing efficiency.<sup>18</sup>

The use of a photonic crystal microresonator as a coupling element on a tip has previously been used to demonstrate TERS.<sup>19</sup> The geometric constraints of the cantilever-based design make the study of opaque samples difficult, and the collinear excitation and residual hole-array transmission do not yet fully eliminate the far-field background. In our

**Received Date:** September 14, 2010

**Accepted Date:** November 9, 2010

**Published on Web Date:** November 19, 2010

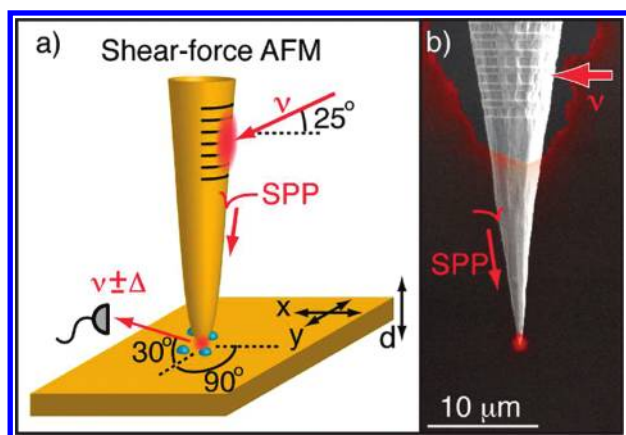


**Figure 1.** (a) Schematic of the experiment. Electrochemically etched Au tips are mounted onto the quartz tuning fork of a shear-force AFM, and a grating is cut using FIB. Incident light is focused onto the grating, and the Raman scattered light excited by the nanofocused SPP at the apex is detected at a  $90^\circ$  angle. (b) SEM micrograph of an electrochemically etched Au tip superimposed with optical image of grating illumination and apex emission.

analogous but simplified approach, we use a grating-coupler<sup>18,20</sup> to launch SPP modes onto the shaft of monolithic Au tips. The conical tips with two-stage optical *mode matching* of the far-field SPP coupling and the mechanisms of adiabatic SPP field concentration into the tip apex represent a unique optical antenna concept for the efficient far-field transduction into nanoscale excitation. With Raman nanospectroscopy of monolayers of dye molecules adsorbed on a Au surface as an example, we demonstrate efficient far-field coupling and propagation-induced nanometer field localization, enabling nanometer spatial resolution for TERS with enhanced sensitivity and contrast and facilitating TERS even with near-IR excitation. This validates the general applicability of the approach, not limited to a specific spectral range, for the implementation of essentially any form of optical spectroscopy in s-SNOM.

In our experiment, a dual noncollinear optical excitation and detection pathway is implemented in a shear-force atomic force microscope (AFM)<sup>12</sup> with side-on illumination of the tip-shaft grating and  $90^\circ$  sagittal detection of the apex scattered light, as shown schematically in Figure 1a. The side-illumination geometry allows the surfaces of thick bulk and nontransparent samples to be studied.<sup>21</sup> Furthermore, compared with contact mode AFM as an alternative to maintain high optical signal duty cycle, shear-force AFM with interaction forces on the order of  $10^2$ 's of pN<sup>22</sup> provides a reduced force perturbation of the sample by several orders of magnitude. The electrochemically etched tips<sup>23,24</sup> are mounted onto the AFM quartz tuning fork, and the grating is fabricated via focused ion beam (FIB) milling, as previously discussed,<sup>25</sup> with the grating period  $a_0$  determined by the in-plane momentum conservation condition  $k_{\text{SPPz}} = k_{\text{in,z}} + nG$ , with integer  $n$  and  $G = 2\pi/a_0$ .

The tip cone angle of  $\sim 15^\circ$  corresponds to a maximum nanofocusing efficiency at  $\approx 800$  nm, yet with broad wavelength range, as theoretically predicted.<sup>26</sup> The SEM image of the Au tip with grating is shown in Figure 1b superimposed with a far-field optical image of grating illumination and apex emission, illustrating the effect of grating-coupling, the

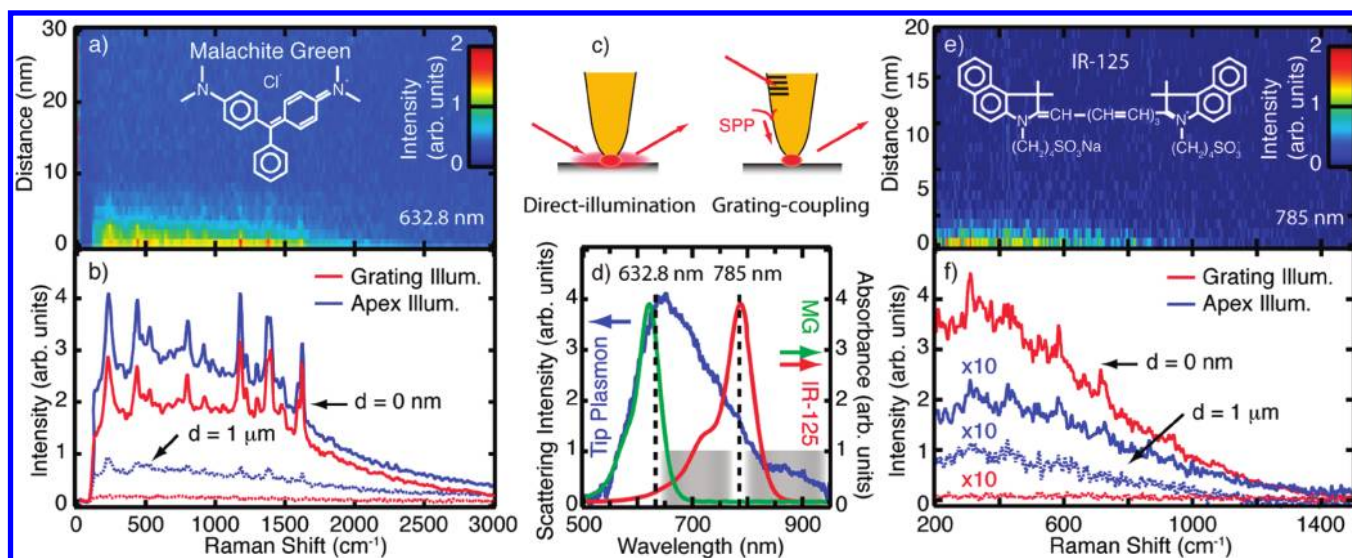
evanescent character of SPP propagation, and the nanoconfined tip apex emission. The tip-scattered Raman light generated by the localized apex plasmon is spectrally filtered and detected using a grating spectrometer (Princeton Instruments). Confocal spatial filtering of the apex emission prevents residual grating-scattered light from reaching the spectrometer. The analyte molecules are deposited by spin coating from solution onto an evaporated Au surface that provides additional field enhancement from plasmonic tip-sample coupling.<sup>12,27,28</sup>

Figure 2a shows TERS results as a function of tip-sample distance<sup>29</sup> for Malachite Green dye on Au with resonant excitation at  $\lambda = 632.8$  nm (He Ne laser) using an incident fluence on the grating of  $F \approx 4.1 \times 10^3$  W/cm<sup>2</sup>. Raman enhancement and spatial localization at distances  $< 10$  nm, with the characteristic peaks of Malachite Green, indicate the near-field origin of the signal. Figure 2b shows a comparison of direct apex illumination TERS (blue) with nanofocusing Raman (red) with the tip in shear-force feedback (solid lines) and retracted  $\sim 1$   $\mu\text{m}$  (dotted lines) under otherwise identical conditions with the same tip.

Although comparable near-field signal levels for both the grating illumination and direct apex illumination TERS are found, the background signal, its origin, and the resulting contrast are fundamentally different. For direct apex illumination, the residual background of the TERS signal with the tip retracted originates from the elliptical diffraction-limited far-field focus with major and minor radii of  $\sim 2$  and  $1$   $\mu\text{m}$ , respectively. In contrast, for grating illumination of the same tip, as illustrated in Figure 2c, no far-field Raman background is observed as a result of the intrinsic nanometer spatial field confinement achieved by the SPP propagation-induced nanofocusing at the apex.<sup>18</sup>

Adiabatic tip-plasmon focusing can readily be extended to longer wavelengths by adjusting the grating parameter and considering cone angle, SPP damping, and other wavelength-related parameters appropriately.<sup>26,30</sup> Performing TERS at long wavelengths is desirable with reduced fluorescence and enhanced sample transparency in biological media. However, the  $\lambda^{-4}$  dependence of Raman scattering<sup>31</sup> greatly diminishes sensitivity. The high nanofocusing efficiency at 800 nm for our cone angles as well as the reduced SPP damping in comparison with 633 nm excitation can compensate the decrease in Raman efficiency. Furthermore, as shown in Figure 2d for a typical tip, this wavelength is within the characteristic range of 600–800 nm for the localized surface plasmon resonances (LSPRs) of the tip apex.<sup>12,27</sup>

Figure 2e shows grating-coupled TERS using 785 nm diode laser excitation ( $F \approx 4.1 \times 10^4$  W/cm<sup>2</sup> at the grating) with  $S_0$ – $S_1$  resonant Raman excitation of a monolayer of the infrared laser dye IR-125<sup>32</sup> (Exciton Inc.) on Au. Figure 2f shows the grating-coupled Raman spectrum at  $d = 0$  nm with the characteristic Raman peaks for IR-125 (red solid line), whereas no spectral features are observed in the corresponding tip-retracted spectrum at  $d \approx 1$   $\mu\text{m}$  (red dotted line). For comparison, standard apex-illuminated TERS acquired with the same tip (solid blue line) exhibits a very low signal intensity with weak spectral features. The Raman response is 20 times weaker than that in the grating coupled case, with a far-field background (blue dotted line) observed with the tip retracted by  $\sim 1$   $\mu\text{m}$ .



**Figure 2.** (a) Grating-coupled TERS distance dependence for  $\lambda = 632.8$  nm of Malachite Green on a Au surface. (b) Corresponding TERS spectra taken with tip in contact (solid line) and tip retracted by  $\sim 1 \mu\text{m}$  (dotted line) for grating-coupled TERS (red) compared with direct apex illumination (blue). (c) Illustration of grating-coupled and direct illumination TERS. (d) Comparison of absorption spectrum of Malachite Green (green) and IR-125 (red) dyes as well as representative tip apex plasmon spectrum (blue). Dashed lines show the excitation wavelengths and the gray bars show the corresponding ranges of Stokes-shifted Raman emission. (e) Grating-coupled TERS with  $\lambda = 785$  nm excitation of IR-125 molecules on Au with (f) comparison of grating illumination (red) and direct apex illumination (blue) with tip in contact (solid line) and tip retracted by  $\sim 1 \mu\text{m}$  (dotted line), demonstrating near-IR TERS as a result of the enhanced focusing efficiency in grating-coupled TERS.

Following established procedures,<sup>33</sup> we can estimate the direct illumination TERS enhancement  $M$  at the apex

$$M = \frac{A_{\text{FF}}}{A_{\text{NF}}} \times \frac{I_{\text{TERS, direct}}}{I_{\text{FF}}} \quad (1)$$

where  $A_{\text{FF}}$  and  $A_{\text{NF}}$  are the areas of the far-field focus and region of near-field enhancement, respectively, and  $I_{\text{TERS, direct}}/I_{\text{FF}}$  is the relative intensity of the TERS signal and far-field background. For direct illumination, from the far-field focus size as stated above for 633 nm excitation and the near-field localization of  $\sim 10$  nm directly obtained from the distance dependence, we determine  $A_{\text{FF}}/A_{\text{NF}} \approx 2 \times 10^4$ . Therefore, with the observed contrast  $I_{\text{TERS, direct}}/I_{\text{FF}} \approx 8$ , this corresponds to  $M \approx 1.6 \times 10^5$ , that is, to a local field enhancement  $L \approx M^{1/4} \approx 20$ .<sup>34</sup> These values fall within the typical range of TERS values for Au tips (see, e.g., ref 33 and references therein), albeit at the lower end of the spectrum, possibly reduced as a result of tip deterioration due to the FIB treatment.

For direct tip illumination at 785 nm, with an observed contrast of  $I_{\text{TERS, direct}}/I_{\text{FF}} \approx 1$  and a larger far- to near-field focus ratio of  $A_{\text{FF}}/A_{\text{NF}} \approx 4.5 \times 10^4$ , this results in a TERS enhancement of  $\sim 4.5 \times 10^4$ . The corresponding weaker field enhancement of  $L \approx 14.6$  is due to a reduced tip-apex plasmon amplitude.

We now turn to the determination of the nanofocusing efficiency. With TERS enhancement occurring on both excitation and scattering, the TERS-scattering process is independent of the excitation method (i.e., grating-coupling or direct illumination). Therefore, any difference in the TERS intensity between the two illumination cases for the same tip is due to a difference in the power of the optical excitation in the near-field region; that is,  $P_{\text{tip, grating}}/P_{\text{tip, direct}} = I_{\text{TERS, grating}}/I_{\text{TERS, direct}}$  with the TERS intensity  $I_{\text{TERS}}$  and the power of the optical

excitation in the near-field region  $P_{\text{tip}}$ . Solving for  $P_{\text{tip, grating}}$  and normalizing to the total incident power  $P_{\text{total}}$ , with the power in the direct illumination near-field excitation being related to the total incident power by  $P_{\text{tip, direct}}/P_{\text{total}} = A_{\text{NF}}/A_{\text{FF}} \times L^2$ , one obtains

$$\frac{P_{\text{tip, grating}}}{P_{\text{total}}} = \frac{A_{\text{NF}}}{A_{\text{FF}}} \times L^2 \times \frac{I_{\text{TERS, grating}}}{I_{\text{TERS, direct}}} \quad (2)$$

For 633 nm illumination, with  $I_{\text{TERS, grating}}/I_{\text{TERS, direct}} \approx 1$  and  $L^2 \approx 400$ , we find  $P_{\text{tip, grating}}/P_{\text{total}} \approx 0.02$ , or equivalently, that the power of the optical excitation in the near-field region beneath the tip is  $\sim 2\%$  of the incident light. The nevertheless comparable TERS signal levels between the direct illumination and grating-coupled cases is a result of the antenna properties of the tip in conventional TERS, with the apex capturing light over a cross-section exceeding its geometric dimensions. For the case of adiabatic nanofocusing, high efficiencies and field enhancements predicted theoretically<sup>16,26</sup> already include the field-enhancement factor of the apex as a result of the transformation of propagating SPPs into localized plasmons. Therefore, even with a grating coupling- and propagation-induced loss of 98%, a signal equivalent to direct-illumination TERS can be achieved.

At 785 nm, with  $I_{\text{TERS, grating}}/I_{\text{TERS, direct}} \approx 20$  and  $L^2 \approx 210$ ,  $P_{\text{tip, grating}}/P_{\text{total}} \approx 0.09$ . Therefore, at 785 nm, 9% of the light incident on the grating is nanofocused into the tip apex region. Consistent with the nonoptimized taper angle and high propagation loss with 633 nm, the nanofocusing efficiency is seen to increase with longer wavelengths.

Nanofocusing is possible over a broad spectral range, determined by the wavelength-dependent SPP damping and related taper angle given by the adiabatic parameter.<sup>16</sup> For our choice of Au tips, guided by established etching

procedures and ambient stability, the SPP propagation length given by  $L = 1/\text{Im}(k_{\text{SPP}})$ , resulting from material damping, imposes a wavelength of  $\lambda \approx 600$  nm as the lower practical limit ( $L \approx 9 \mu\text{m}$ ),<sup>55</sup> for silver tips, wavelengths down to  $\lambda \approx 400$  nm can be used ( $L \approx 10 \mu\text{m}$  for  $\lambda = 400$  nm). For longer wavelength, the increase in propagation lengths (e.g. Au:  $L \approx 85 \mu\text{m}$  for  $\lambda = 800$  nm) benefits contrast and experimental simplicity; however, the adiabatic condition dictates the need for increasingly slender waveguide tapers, providing a practical challenge for the extension into the mid-IR.<sup>56</sup>

The efficiency of conventional TERS relies solely on the enhancement and scattering cross section of the tip apex. In contrast, in nano-Raman spectroscopy by adiabatic tip-plasmon focusing, the grating segment acts as a receiving antenna that can be mode-matched to the spatially separated localized tip apex SPP via the focusing waveguide properties of the conical tip shaft. This opens the possibility for the independent optimization of maximum field concentration (depending, e.g., on cone angle) and localized apex plasmon resonance conditions (depending on apex geometry). Further improvement in the mode-matching can be achieved by reducing the losses resulting from SPP propagation, waveguide cutoff, reflection, and scattering from grating corrugation or shaft roughness.

In spectroscopy in general, and particularly for nanospectroscopy, the fundamental limit to sensitivity and emitter localization is often determined by the contrast (near-field to background signal ratio), where the background level is frequently difficult to remove. In TERS, the near- to far-field signal contrast is directly related to the degree and spatial extent of the near-field enhancement region relative to the far-field focus size. A high contrast and suppression of the far-field background can be achieved in various TERS geometries with a combination of large field enhancement and the use of high-NA optics, and can be further benefitted by spatially dispersed sample material,<sup>13,37–41</sup> yet is still practically constrained by the diffraction limit. In grating-coupling TERS, the far-field signal is negligible and principally of a different nature as a consequence of the nonlocal excitation with no direct far-field sample irradiation and the effective suppression of any residual grating-scattered light via confocal spatial filtering. It is of note that the unique background suppression mechanism of grating-coupled TERS is effective without the need for high-NA optics or large field-enhancement values.

In grating-coupling, the far-field emission and sample illumination by fundamental excitation light from the point source at the tip apex would, in principle, be capable of generating a far-field Raman background within the confocal detection focus. However with the tip positioned a few nanometers from the substrate and the apex excitation represented by a local point dipole oriented along the tip axis, as shown before,<sup>18</sup> far-field irradiation occurs at grazing incidence with respect to the sample plane.

Further improvement in the technique can be achieved by refining the excitation and detection geometry, particularly the use of confocal filtering in combination with a high-NA objective in an axial detection scheme, as well as optimized grating parameters, incident angle, and apex-grating separation distance. It should be noted, however, that details of the

tip-sample coupling responsible for efficient TERS generation are highly complex. This can, for example, result in a loss of excitation enhancement due to the broad  $k$ -vector distribution at the apex allowing for launching propagating SPPs at the sample surface, as suggested by reduced fundamental apex emission observed upon approach of a Au surface (data not shown).<sup>18</sup>

Although the enhanced TERS performance in grating-coupling originates from adiabatic SPP nanofocusing, a qualitatively new physical mechanism, the experimental implementation does not require substantial modification of a conventional shear-force or STM-based TERS configuration. Alternatively, conventional cantilever AFM tips can be used after metal coating. Through the use of a compatible high-NA axial detection scheme for transparent samples, improved signal collection can be achieved. While possible in general, the application in liquid environments will require the modification of grating parameters or incident angle for efficient grating-coupling, whereas SPPs propagating across a liquid-air interface for tips immersed in thin liquid layers can possibly experience scattering and reflection losses. The use of the new approach is expected to be especially beneficial for the study of, for example, bulk crystalline samples<sup>42</sup> or biological systems,<sup>43</sup> where the far-field Raman background originating from the direct apex illumination can eclipse or obfuscate the TERS signal. Here effective background suppression could lead to significant improvement in the utility of near-field Raman spectroscopy.

In conclusion, we have demonstrated the application of adiabatic plasmon nanofocusing in monolithic Au scanning probe tips for TERS. The high nanofocusing efficiency allows for the extension of TERS into the near-IR, as demonstrated for  $\lambda = 800$  nm. The spatial separation of the far-field grating-coupling of the pump radiation and the propagation-induced near-field apex localization allows for an improvement in near- to far-field contrast in TERS with effective suppression of the far-field background with multiple excitation wavelengths. This capability for nonlocal generation of a nanoscale excitation source with true nanofocusing efficiency and intrinsic background suppression holds promise for a wide range of spectroscopic techniques. Potential applications of remote excitation near-field spectroscopy beyond TERS range from *s*-SNOM implementations without the need for signal demodulation<sup>18</sup> and background-free near-field luminescence spectroscopy to the full spatial and temporal control over optical fields on the nanoscale for nonlinear and ultrafast nanospectroscopy.<sup>44</sup>

## AUTHOR INFORMATION

### Corresponding Author:

\*To whom correspondence should be addressed. E-mail: markus.raschke@colorado.edu.

### Present Addresses:

<sup>§</sup> Department of Physics and JILA, University of Colorado, Boulder, CO, 80309.

**ACKNOWLEDGMENT** A portion of this research was performed using EMSL, a national scientific user facility sponsored by the

Department of Energy's Office of Biological and Environmental Research and located at Pacific Northwest National Laboratory. We also acknowledge the support provided by Princeton Instruments.

## REFERENCES

- Betzig, E.; Patterson, G. H.; Sougat, R.; Lindwasser, O. W.; Olenych, S.; Bonifacio, J. S.; Davidson, M. W.; Lippencott-Schwartz, J.; Hess, H. F. Imaging Intracellular Fluorescent Proteins at Nanometer Resolution. *Science* **2006**, *313*, 1642–1645.
- Hell, S. W.; Wichmann, J. Breaking the Diffraction Resolution Limit by Stimulated Emission: Stimulated-Emission-Depletion Fluorescence Microscopy. *Opt. Lett.* **1994**, *19*, 780–782.
- Betzig, E.; Trautman, J. K.; Harris, T. D.; Weiner, J. S.; Kostelak, R. L. Breaking the Diffraction Barrier: Optical Microscopy on a Nanometric Scale. *Science* **1991**, *251*, 1468–1470.
- Hecht, B.; Beilefeldt, H.; Inouye, Y.; Pohl, D. W.; Novotny, L. Facts and Artifacts in Near-Field Optical Microscopy. *J. Appl. Phys.* **1997**, *81*, 2492–2498.
- Keilmann, F.; Hillenbrand, R. Near-Field Microscopy by Elastic Light Scattering from a Tip. *Philos. Trans. R. Soc. London, Ser. A* **2004**, *362*, 787–805.
- Yano, T.; Verma, P.; Saito, Y.; Ichimura, T.; Kawata, S. Pressure-Assisted Tip-Enhanced Raman Imaging at a Resolution of a Few Nanometres. *Nature Photon* **2009**, *3*, 473–477.
- Taubner, T.; Hillenbrand, R.; Keilmann, F. Nanoscale Polymer Recognition by Spectral Signature in Scattering Infrared Near-Field Microscopy. *Appl. Phys. Lett.* **2004**, *85*, 5064–5066.
- Raschke, M. B.; Molina, L.; Elsaesser, T.; Kim, D. H.; Knoll, W.; Hinrichs, K. Apertureless Near-Field Vibrational Imaging of Block-Copolymer Nanostructures with Ultrahigh Spatial Resolution. *ChemPhysChem* **2005**, *6*, 2197–2203.
- Ichimura, T.; Hayazawa, N.; Hashimoto, M.; Inouye, Y.; Kawata, S. Tip-Enhanced Coherent Anti-Stokes Raman Scattering for Vibrational Nanoimaging. *Phys. Rev. Lett.* **2004**, *92*, 220801.
- Hartschuh, A.; Sanchez, E. J.; Xie, X. S.; Novotny, L. High-Resolution Near-Field Raman Microscopy of Single-Walled Carbon Nanotubes. *Phys. Rev. Lett.* **2003**, *90*, 095503.
- Stöckle, R. M.; Suh, Y. D.; Deckert, V.; Zenobi, R. Nanoscale Chemical Analysis by Tip-Enhanced Raman Spectroscopy. *Chem. Phys. Lett.* **2000**, *318*, 131–136.
- Neacsu, C. C.; Dreyer, J.; Behr, N.; Raschke, M. B. Scanning-Probe Raman Spectroscopy with Single-Molecule Sensitivity. *Phys. Rev. B* **2006**, *73*, 193406.
- Steidtner, J.; Pettinger, B. Tip-Enhanced Raman Spectroscopy and Microscopy on Single Dye Molecules with 15 nm Resolution. *Phys. Rev. Lett.* **2008**, *100*, 236101.
- Nakayama, Y.; Pauzauskis, P. J.; Radenovic, A.; Onorato, R. M.; Saykally, R. J.; Liphardt, P.; Yang, P. Tunable Nanowire Nonlinear Optical Probe. *Nature* **2007**, *447*, 1098–1102.
- Palomba, S.; Novotny, L. Near-Field Imaging with a Localized Nonlinear Light Source. *Nano Lett.* **2009**, *9*, 3801–3805.
- Stockman, M. I. Nanofocusing of Optical Energy in Tapered Plasmonic Waveguides. *Phys. Rev. Lett.* **2004**, *93*, 137404.
- Babadjanyan, A. J.; Margaryan, N. L.; Nerkararyan, K. V. Superfocusing of Surface Polaritons in the Conical Structure. *J. Appl. Phys.* **2000**, *87*, 3785–3788.
- Neacsu, C. C.; Berweger, S.; Olmon, R. L.; Saraf, L. V.; Ropers, C.; Raschke, M. B. Near-Field Localization in Plasmonic Superfocusing: A Nanoemitter on a Tip. *Nano Lett.* **2010**, *10*, 592–596.
- De Angelis, F.; Das, G.; Candeloro, P.; Patrini, M.; Galli, M.; Bek, A.; Lazzarino, M.; Maksymov, I.; Liberale, C.; Andreani, L. C.; Di Fabrizio, E. Nanoscale Chemical Mapping Using Three-Dimensional Adiabatic Compression of Surface Plasmon Polaritons. *Nat. Nanotechnol.* **2009**, *5*, 67–72.
- Raether, H. *Surface Plasmons on Smooth and Rough Surfaces and on Gratings*; Springer-Verlag: New York, 1988.
- Berweger, S.; Raschke, M. B. Signal Limitations in Tip-Enhanced Raman Scattering: The Challenge to Become a Routine Analytical Technique. *Anal. Bioanal. Chem.* **2009**, *396*, 1613–1621.
- Karrai, K.; Grober, R. D. Piezoelectric Tip-Sample Distance Control for Near Field Optical Microscopes. *Appl. Phys. Lett.* **1995**, *66*, 1842–1844.
- Ren, B.; Picardi, G.; Pettinger, B. Preparation of Gold Tips Suitable for Tip-Enhanced Raman Spectroscopy and Light Emission by Electrochemical Etching. *Rev. Sci. Instrum.* **2004**, *75*, 837–841.
- Wang, X.; Liu, Z.; Zhuang, M.-D.; Zhang, H.-M.; Wang, X.; Xie, Z.-X.; Wu, D.-Y.; Ren, B.; Tian, Z.-Q. Tip-Enhanced Raman Spectroscopy for Investigating Adsorbed Species on a Single-Crystal Surface Using Electrochemically Prepared Au Tips. *Appl. Phys. Lett.* **2007**, *91*, 101105.
- Ropers, C.; Neacsu, C. C.; Elsaesser, T.; Albrecht, M.; Raschke, M. B.; Lienau, C. Grating-Coupling of Surface Plasmons onto Metallic Tips: A Nanoconfined Light Source. *Nano Lett.* **2007**, *7*, 2784–2788.
- Issa, N. A.; Guckenberger, R. Optical Nanofocusing on Tapered Metallic Waveguides. *Plasmonics* **2007**, *2*, 31–37.
- Neacsu, C. C.; Steudle, G. A.; Raschke, M. B. Plasmonic Light Scattering from Nanoscopic Metal Tips. *Appl. Phys. B: Lasers Opt.* **2005**, *80*, 295–300.
- Behr, N.; Raschke, M. B. Optical Antenna Properties of Scanning Probe Tips: Plasmonic Light Scattering, Tip-Sample Coupling, and Near-Field Enhancement. *J. Phys. Chem. C* **2008**, *112*, 3766–3773.
- Here zero distance is defined as a ~25% decrease in the tuning fork oscillation amplitude. This corresponds to a physical tip-sample distance of ~5 nm.
- Gramotnev, D. K.; Vogel, M. W.; Stockman, M. I. Optimized Nonadiabatic Nanofocusing of Plasmons by Tapered Metal Rods. *J. Appl. Phys.* **2008**, *104*, 034311.
- Wilson, E. B.; Decius, J. C.; Cross, P. C. *Molecular Vibrations: The Theory of Infrared and Raman Vibrational Spectra*; Dover Publications: New York, 1955.
- 2-[7-[1,3-Dihydro-1,1-dimethyl-3-(4-sulfobutyl)-2H-benz[e]indol-2-ylidene]-1,3,5-heptatrienyl]-1,1-dimethyl-3-(4-sulfobutyl)-1H-benz[e]indolium hydroxide.
- Roy, D.; Wang, J.; Williams, C. Novel Methodology for Estimating the Enhancement Factor for Tip-Enhanced Raman Spectroscopy. *J. Appl. Phys.* **2009**, *105*, 013530.
- Because of the broad plasmon linewidths observed for our tips compared with the Raman shift, we approximate the enhancement of the incident and tip-scattered light by the tip to be equal.
- Johnson, P. B.; Christy, R. W. Optical Constants of the Noble Metals. *Phys. Rev. B* **1972**, *6*, 4370–4379.
- Maier, S. A.; Andrews, S. R.; Martin-Moreno, L.; García-Vidal, F. J. Terahertz Surface Plasmon-Polariton Propagation and Focusing on Periodically Corrugated Metal Wires. *Phys. Rev. Lett.* **2006**, *97*, 176805.
- Pettinger, B.; Ren, B.; Picardi, G.; Schuster, R.; Ertl, G. Nanoscale Probing of Adsorbed Species by Tip-Enhanced Raman Spectroscopy. *Phys. Rev. Lett.* **2004**, *92*, 096101.

- (38) Zhang, D.; Wang, X.; Braun, K.; Egelhaaf, H.-J.; Fleischer, M.; Hennemann, L.; Hintz, H.; Stanciu, C.; Brabec, C. J.; Kern, D. P.; Meixner, A. J. Parabolic Mirror-Assisted Tip-Enhanced Spectroscopic Imaging for Non-Transparent Materials. *J. Raman Spectrosc.* **2009**, *40*, 1371–1376.
- (39) Bailo, E.; Deckert, V. Tip-Enhanced Raman Spectroscopy of Single RNA Strands: Towards a Novel Direct-Sequencing Method. *Angew. Chem. Int. Ed.* **2008**, *47*, 1658–1661.
- (40) Zhang, W.; Yeo, B. S.; Schmid, T.; Zenobi, R. Single Molecule Tip-Enhanced Raman Spectroscopy with Silver Tips. *J. Phys. Chem. C* **2007**, *111*, 1733–1738.
- (41) Ichimura, T.; Watanabe, H.; Morita, Y.; Verma, P.; Kawata, S.; Inouye, Y. Temporal Fluctuation of Tip-Enhanced Raman Spectra of Adenine Molecules. *J. Phys. Chem. C* **2007**, *111*, 9460–9464.
- (42) Ossikovski, R.; Nguyen, Q.; Picardi, G. Simple Model for the Polarization Effects in Tip-Enhanced Raman Spectroscopy. *Phys. Rev. B* **2007**, *75*, 045412.
- (43) Yeo, B.-S.; Mädler, S.; Schmid, T.; Zhang, W.; Zenobi, R. Tip-Enhanced Raman Spectroscopy Can See More: The Case of Cytochrome C. *J. Phys. Chem. C* **2008**, *112*, 4867–4873.
- (44) Durach, M.; Rusina, A.; Stockman, M. I.; Nelson, K. Toward Full Spatiotemporal Control on the Nanoscale. *Nano Lett.* **2007**, *7*, 3145–3149.